



HAL
open science

Efficiency of four-wave mixing between orthogonally polarized linear waves and solitons in a birefringent fiber

C Mas Arabí, F. Bessin, Alexandre Kudlinski, Arnaud Mussot, D. Skryabin,
Matteo Conforti

► **To cite this version:**

C Mas Arabí, F. Bessin, Alexandre Kudlinski, Arnaud Mussot, D. Skryabin, et al.. Efficiency of four-wave mixing between orthogonally polarized linear waves and solitons in a birefringent fiber. *Physical Review A*, 2016, 94 (6), 10.1103/PhysRevA.94.063847 . hal-02386609

HAL Id: hal-02386609

<https://hal.science/hal-02386609>

Submitted on 29 Nov 2019

HAL is a multi-disciplinary open access archive for the deposit and dissemination of scientific research documents, whether they are published or not. The documents may come from teaching and research institutions in France or abroad, or from public or private research centers.

L'archive ouverte pluridisciplinaire **HAL**, est destinée au dépôt et à la diffusion de documents scientifiques de niveau recherche, publiés ou non, émanant des établissements d'enseignement et de recherche français ou étrangers, des laboratoires publics ou privés.

Efficiency of four-wave mixing between orthogonally polarized linear waves and solitons in a birefringent fiber

C. Mas Arabi,¹ F. Bessin,¹ A. Kudlinski,¹ A. Mussot,¹ D. Skryabin,^{2,3} and M. Conforti¹

¹*Univ. Lille, CNRS, UMR 8523-PhLAM-Physique des Lasers Atomes et Molécules, F-59000 Lille, France*

²*Department of Physics, University of Bath, Bath, UK*

³*ITMO University, Kronverksky Avenue 49, St. Petersburg 197101, Russian Federation*

(Dated: November 28, 2016)

We analyze the interaction between orthogonally polarized solitons and dispersive waves via four-wave mixing in a birefringent fiber. We calculate analytically the efficiency of the phase-sensitive scattering between orthogonally polarized soliton and dispersive wave. Experiments performed by using a photonic crystal fiber perfectly match the analytical predictions.

I. INTRODUCTION

The interaction between solitons and dispersive waves (DWs) in optical waveguides is an active field of research. These phenomena typically take place during the process of supercontinuum generation [1], making their deep understanding relevant for the design of broadband sources. These interactions have been proposed as a candidate to optical switching [2], as a close analogy with event horizon in black holes [3, 4] and for the trapping of DWs in a cavity-like soliton pair [5–7]. Classically, these interactions were fundamentally studied in the case of bright fundamental solitons, but recently, it has been found that other kinds of solitons can interact with linear waves through this mechanism such as dark [8] and higher order solitons [9].

Physically, the scattering of a DW on a soliton can be understood as a four-wave mixing (FWM) process [10–12], which, under appropriate conditions, gives birth to new spectral components. Two different kinds of soliton/DW interaction can take place: in the first one, called non-phase sensitive, the moving refractive index variation produced by the soliton itself is able to generate new spectral components via cross-phase modulation (XPM). The frequencies of these bands do not explicitly depend on the soliton phase. The second type, called phase-sensitive [13], involves a genuine FWM process between the soliton and the dispersive wave, which generates new spectral bands whose frequencies directly depend on the soliton phase [13, 14]. The efficiency of these interactions depends on the frequency of the involved waves, the spectral width of the soliton and the group velocity difference between the waves. In the case of non-phase sensitive resonance, the efficiency has been calculated analytically [12, 15, 16], whereas, in the case of phase-sensitive process, a full theoretical understanding is still missing.

The main goal of this paper is to characterize theoretically and experimentally the phase-sensitive interaction between solitons and DWs and demonstrate conditions providing maximal power of the generated signal. We consider the collision between a soliton and a weak continuous wave (CW) orthogonally polarized in a birefringent fiber. In this case the frequency of the waves gen-

erated by the phase-sensitive and phase-insensitive scattering can be unambiguously identified. The article is organized as follows. In Sec. II we present the analytical calculations of the efficiency of the phase-sensitive process. In Sec. III we describe the experimental results and compare them with the theory. Conclusions are drawn in Sec. IV.

II. THEORY

The evolution of the two linear polarization components along a birefringent fiber can be described by means of two coherently coupled nonlinear Schrödinger equations [17]:

$$i\partial_z A_{x,y} + D_{x,y}(i\partial_t)A_{x,y} + \gamma[|A_{x,y}|^2 + \frac{2}{3}|A_{y,x}|^2]A_{x,y} + \frac{\gamma}{3}A_{x,y}^*A_{y,x}^2 = 0. \quad (1)$$

The dispersion operators are defined as:

$$D_x(i\partial_t) = \sum_{n \geq 2} \frac{\beta_{nx}}{n!} (i\partial_t)^n, \quad (2)$$

$$D_y(i\partial_t) = \Delta\beta_0 + \Delta\beta_1 i\partial_t + \sum_{n \geq 2} \frac{\beta_{ny}}{n!} (i\partial_t)^n, \quad (3)$$

where $\beta_n = \partial_\omega^n \beta(\omega)|_{\omega=\omega_0}$, $\Delta\beta_0 = \beta_{0y} - \beta_{0x}$, $\Delta\beta_1 = \beta_{1y} - \beta_{1x}$. We consider $\beta_{0y} > \beta_{0x}$ so that x is the fast axis, according to the usual terminology. Here, $A_{x,y}$ are the field envelopes polarized along the fiber neutral axes x and y , respectively, z is the longitudinal coordinate, and γ is the nonlinear coefficient. The characteristics (power and duration) of the pulses considered here permits to safely neglect the Raman and self-steepening effects.

We study the propagation along the fiber of a soliton polarized along the x (fast) axis $A_x = \sqrt{P_0} \text{sech}(t/T_0) e^{iqz}$ ($q = \gamma P_0/2$) with frequency ω_0 , together with a weak continuous wave $A_y = g$ polarized along the y (slow) axis with frequency ω_p , that we term the pump, following the terminology of Refs. [10, 13].

We report in Figure 1 a typical example of the interaction under investigation in this paper. We considered a 3 m-long photonic crystal fiber (PCF), whose parameters

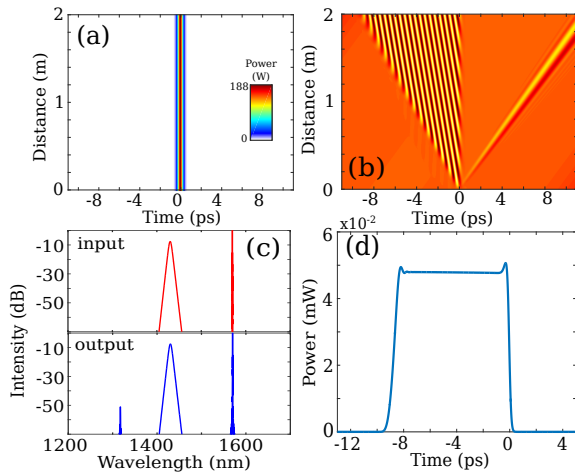


FIG. 1. Collision between a soliton and a CW. (a),(b) Spatiotemporal evolutions of the x and y components, respectively, obtained from numerical solution of Eqs. (1). (c) Total input (top) and output (bottom) spectrum. (d) Temporal profile of the generated pulse at 1318 nm. Simulation parameters: see text.

at 1430 nm are $\Delta\beta_0 = 295 \text{ m}^{-1}$, $\Delta\beta_1 = -0.4 \text{ ps}\cdot\text{m}^{-1}$, $\beta_{2x} \approx \beta_{2y} = -4.5 \times 10^{-26} \text{ s}^2/\text{m}$ and $\gamma = 5 \text{ W}^{-1}\cdot\text{km}^{-1}$, corresponding to the PCF used in experiments hereafter. Dispersion terms of order higher than 2 turn out to be irrelevant, and have been neglected. It is worth noting that, despite the high value of $\Delta\beta_0$, coherent terms $A_{x,y}^* A_{y,x}^2$ in Eq. (1) are not negligible. For example, they can be perfectly phase-matched for a soliton and a CW located around 1430 nm and 1570 nm, respectively.

Figures 1 (a),(b) show the evolution along the fiber of the field intensity in time domain for the x and y polarizations. The input fundamental soliton, of peak power $P_0 = 188 \text{ W}$ ($\mathbf{q} = \mathbf{0.47} \text{ m}^{-1}$), duration $T_0 = 0.21 \text{ ps}$, wavelength $\lambda_0 = 1430 \text{ nm}$, propagates without deformation, and is almost not perturbed by the collision with the y -polarized linear wave, as shown in Fig. 1 (a). The CW has an average power of 0.1 W and central wavelength $\lambda_p = 1570 \text{ nm}$. As shown in Fig. 1 (b), during the interaction with the soliton, a part of the CW is reflected and propagates with a different group velocity, corresponding to a new generated spectral component around 1318 nm, as can be seen from the output spectrum reported in Fig. 1 (c). The temporal profile of this new spectral component shown in Fig. 1 (d) (**obtained by filtering-out the CW pump from the output pulse polarized along the y-axis**) is a square-like pulse of duration T_g . A small quantity of radiation is also emitted at the very beginning of the process [see Fig. 1 (b)], which rapidly begins and does not play any role.

The numerical simulation clearly indicates that the soliton does not experience any dynamics, since it is not perturbed by the collision, nor it is emitting Cherenkov radiation [18], due to the negligible value of β_3 at the soliton wavelength. Therefore, we can assume that

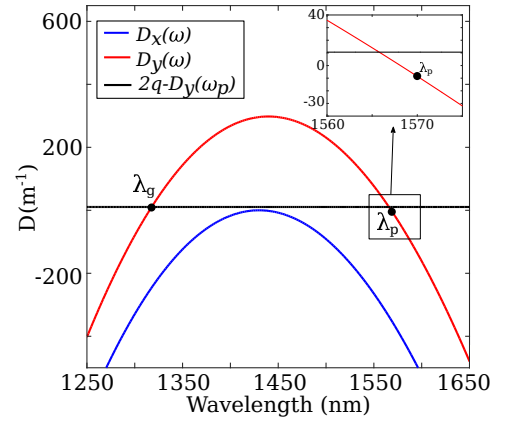


FIG. 2. Phase-matching diagram: graphical solution of Eq. (6). Upper (lower) curve correspond to linear dispersion in the y -axis (x -axis). Horizontal line correspond to equation (6). Parameters as in Fig. 1.

$A_x(z, t) = F(t)e^{iqz} = \sqrt{P_0}\text{sech}(t/T_0)e^{iqz}$ in Eq. (1), and linearize for $|g| \ll |A_x|$, to get the following evolution equation for the y component:

$$i\partial_z g + D_y(i\partial_t)g + \frac{\gamma}{3}(2|F|^2 g + F^2 g^* e^{i2qz}) = 0. \quad (4)$$

We can write the field g as the sum of the cw pump and the generated wave:

$$g = W e^{i(k_p z - \omega_p t)} + u(z, t) e^{i(k_g z - \omega_g t)}, \quad (5)$$

where $k_{g,p} = D_y(\omega_{g,p})$. The generated frequency ω_g , such that $k_g = D_y(\omega_g)$, can be found from the phase-matching conditions [11–13]:

$$D_y(\omega) = 2q - D_y(\omega_p), \quad (6)$$

$$D_y(\omega) = D_y(\omega_p), \quad (7)$$

where $D_y(\omega) = \Delta\beta_0 + \Delta\beta_1\omega + \sum_{n \geq 2} \beta_{ny} \omega^n / n!$ is the dispersion operator (3) in frequency domain. Equation (6) is the phase-sensitive phase-matching condition, which describes FWM between the soliton and the CW pump. Equation (7) is the non phase-sensitive phase-matching condition describing an XPM process and it does not depend explicitly on soliton parameters. Figure 2 (a) displays the phase-matching diagram [graphical solution of Eq. (6)]. The red (upper) curve corresponding to $D_y(\omega)$ shows that a soliton at 1430 nm (at the top of the blue (lower) curve) and a CW pump at 1570 nm generate a wave at 1318 nm (at the intersection with the black (horizontal) line). The phase-insensitive process is inefficient and no spectral component associated to it can be generated. As we want to study the FWM process, we require that the perturbation field satisfies the condition (6).

By inserting the Ansatz (5) into Eq. (4), and assuming that the generated wave is spectrally narrow, so that one only account for the first order dispersion, we get:

$$i\partial_z u + iD'_g \partial_t u + \frac{\gamma}{3}(2|F|^2 u + F^2 W^* e^{i\Delta\omega t}) = 0, \quad (8)$$

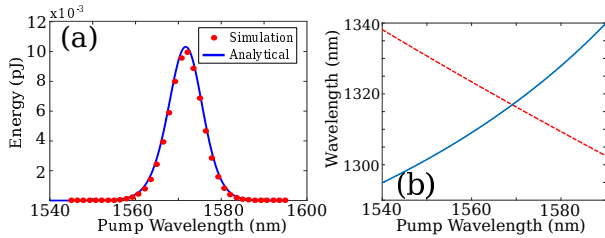


FIG. 3. (a) Energy of the generated wave as a function of cw pump wavelength. Solid blue curve and red dots stand for theoretical [Eq. (12)] and numerical results. (b) Red (dashed) curve: wavelength at which $2\omega_0 = \omega_p + \omega_g$ (energy conservation), as a function of cw pump wavelength. Blue (solid) curve: wavelength at which phase-sensitive phase-matching is satisfied [Eq. (6)], as a function of cw pump wavelength. Parameters as in Fig. 1.

where we have defined $\Delta\omega = \omega_g + \omega_p - 2\omega_0$, and $D'_{p,g} = \partial_\omega D_y(\omega)|_{\omega_p, \omega_g}$. The forcing term $|F|^2 u$ in Eq. (8) can be disregarded if we assume that the generated wave is small ($|u| \ll |w$):

$$i\partial_z u + iD'_g \partial_t u + \frac{\gamma}{3} F^2 W^* e^{i\Delta\omega t} = 0. \quad (9)$$

Equation (9) can be easily solved:

$$u(\tau, z) = \frac{i\gamma}{3} \int_0^z W^* F^2(\tau, s) e^{i\Delta\omega(\tau + D'_g s)} ds \quad (10)$$

with $\tau = t - D'_g z$. The integral in Eq. (10) can be calculated explicitly since we have considered a cw pump ($W = \sqrt{P_p}$):

$$\begin{aligned} u &= \frac{i\gamma\sqrt{P_p}P_0}{3D'_g} \int_{t-D'_g z}^t \text{sech}^2\left(\frac{t'}{T_0}\right) e^{i\Delta\omega t'} dt' \approx \\ &\approx \frac{i\gamma\sqrt{P_p}P_0}{3|D'_g|} \int_{-\infty}^{\infty} \text{sech}^2\left(\frac{t'}{T_0}\right) e^{i\Delta\omega t'} dt' = \\ &= \frac{\pi\gamma\Delta\omega P_{sol}\sqrt{P_p}T_0^2}{3|D'_g|} \sinh^{-1}\left(\frac{\Delta\omega T_0\pi}{2}\right). \end{aligned} \quad (11)$$

Supposing that the generated wave amplitude stays constant, the energy of the generated pulse can be approximated as $E_g = |u|^2 T_g$, where the duration T_g is calculated as $T_g = (L_{fiber}/D'_g)$. We get

$$E_g = P_p \left(\frac{|\beta_{2x}|\Delta\omega\pi}{3} \right)^2 \sinh^{-2}\left(\frac{\Delta\omega T_0\pi}{2}\right) \frac{L_{fiber}}{D'_g}, \quad (12)$$

where we have used $P_{sol} = |\beta_{2x}|/(\gamma T_0^2)$.

The maximal generated wave energy is attained when the condition $\Delta\omega = 0$ is satisfied, i.e. when $2\omega_0 = \omega_p + \omega_g$. This states the conservation of energy for the degenerate FWM process between the soliton, pump and generated wave. This condition is complemented by the phase-matching relation Eq. (6), so that the conversion is maximal when both energy and momentum are conserved

during the scattering process. Figure 3(a) shows an example of generated wave energy as a function of pump wavelength. The maximum is reached around 1570 nm, where energy and momentum are conserved at the same time, as shown in Fig. 3(b). Figure 3(a) shows a comparison between numerical simulations and the theory. The agreement between numerical (red dots) and analytical result (blue (solid) curve) obtained by using Eq. (12) is excellent.

The frequency at which the generation is maximal is:

$$\omega_g = -\sqrt{\frac{2(q - \Delta\beta_0)}{\beta_{2x}}}. \quad (13)$$

In the case of a quite highly birefringent fiber, $\Delta\beta_0 \gg q$ and $\beta_{2x} < 0$, therefore only solitons polarized along the fast axis can fulfill both energy and momentum conservation. It is important to note that, as it was shown in Refs. [19, 20], a soliton polarized along the fast axis can be unstable if a power threshold is reached. Soliton dynamics in this regime and its stability were studied in Refs. [21–24]. In all the cases we consider, the soliton power is well below the instability threshold.

III. EXPERIMENTS

Figure 4 displays the experimental setup that we have built to study the conversion efficiency of the FWM process. The soliton is excited using gaussian pulses of 250 fs full width at half maximum (FWHM) duration centered at 1430 nm delivered from an optical parametric oscillator (OPO) pumped by a Ti:Sa laser. A variable attenuator made of a half-wave plate and a polarizer is placed at the OPO exit and allows to finely adjust the input power. An additional half-wave plate allows to orientate the incident polarization state on the beam splitter so that transmission is maximized. To generate the CW pump, we use a CW laser diode tunable in the range 1540-1600 nm. This radiation is then amplified using an erbium doped fiber amplifier. A half-wave plate placed just after sets the polarization state orthogonal to the one of the first beam. After the two beams are combined using the beam splitter, a final half-wave plate is used to align both orthogonally polarized beams to the polarization axes of the PCF. Care is taken to launch the short pulse exciting the soliton on the fast axis and the CW pump on the slow axis. The PCF has a group birefringence of 1.2×10^{-4} at 1430 nm. At this wavelength, it exhibits large anomalous group velocity dispersion which equals $\beta_2 = -4.5 \times 10^{-26} \text{ s}^2/\text{m}$. The nonlinear coefficient is $\gamma = 5 \text{ W}^{-1} \times \text{km}^{-1}$.

The input power of gaussian pulses was carefully adjusted in order to excite a fundamental soliton. This was checked from autocorrelation measurements at the fiber output [see example in Fig. 4(b)], which gave a duration of $T_0 = 133 \text{ fs}$ for the fundamental soliton. A typical output spectrum in the presence of both the soliton (centered

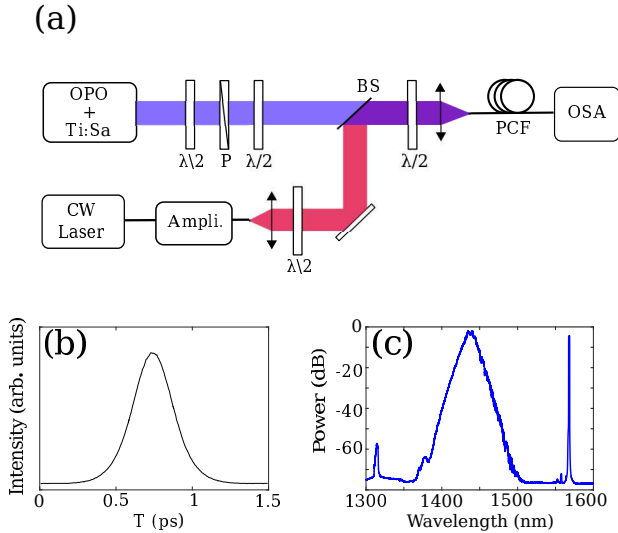


FIG. 4. (a) Experimental setup. OPO: optical parametric oscillator; BS: beam splitter; P: polarizer; $\lambda/2$: half-wave plate; Ampli: amplifier; OSA: optical spectrum analyzer. (b) Autocorrelation trace of the soliton after propagation in the 3 m-long PCF. (c) Typical output spectrum after amplified spontaneous emission (ASE) filtering.

at 1430 nm) and the CW pump (located at 1570 nm) is displayed in Fig. 4(c). In addition to these two spectral peaks, the wave generated through the phase-sensitive FWM was observed at 1317 nm, in excellent agreement with the predictions Eq. (6). Additional measurements not reported here showed that the generated wave is polarized along the slow axis, as predicted by the theory.

As a next step of our study we have verified the validity of Eq. (12) and measured the energy of the generated wave, E_g , as a function of the pump wavelength. In experiments, E_g is measured by directly integrating the output spectrum. However, only a small fraction of the pump effectively interacts with the soliton over a finite fiber length L_{fiber} . To take this into account, we introduce a conversion efficiency η as follows [15]:

$$\eta = \lim_{T_p \rightarrow +\infty} \frac{|u|^2 T_g}{P_p T_p} = \left(\frac{\beta_{2x} \Delta \omega \pi}{3 D'_g} \right)^2 \sinh^{-2} \left(\frac{\Delta \omega \pi T_0}{2} \right) \frac{D'_g}{D'_p}, \quad (14)$$

where $T_p = L_f / D'_p$ is the duration of the part of the pump that has effectively interacted with the soliton over the fiber length L_{fiber} .

Figure 5, shows the results from Eq. (14), assuming a soliton duration T_0 of 133 fs (blue (solid) curve), together with the experimental recordings (black dots). There is a good agreement between the numerical and experimental data.

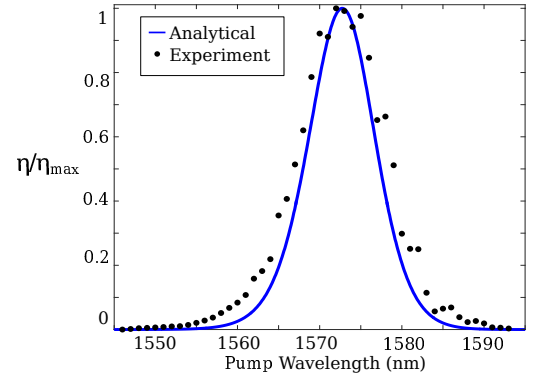


FIG. 5. Comparison between theoretical (blue (solid) curve, Eq. (14)) and experimentally measured (black dots) conversion efficiency. Soliton duration $T_0 = 133$ fs; other parameters as in Fig. 1.

IV. CONCLUSIONS

We developed a theory predicting the efficiency of generation of new frequencies due to the phase-sensitive FWM process between a soliton and an orthogonally polarized CW. Our theoretical predictions have been fully validated by numerical simulations as well as by the experimental measurement performed in a birefringent PCF. This study contributes to a further understanding of the rich dynamics related to soliton interaction with pulsed or continuous waves that is expected to occur in highly nonlinear and complex phenomena such as super-continuum generation or rogue wave formation.

V. ACKNOWLEDGMENTS

We acknowledge fruitful discussions with Stefano Trillo. The present research was partially supported by IRCICA (USR 3380 CNRS), by the Agence Nationale de la Recherche in the framework of the Labex CEMPI (ANR-11-LABX-0007-01), Equipex FLUX (ANR-11-EQPX-0017), by the projects NoAWE (ANR-14-ACHN-0014), TOPWAVE (ANR-13-JS04-0004), by the CPER Photonics for Society and by the Russian Foundation for Basic Research (RFBR).

[1] D. V. Skryabin and A.V. Gorbach, Colloquium: Looking at a soliton through the prism of optical super-continuum, Rev. Mod. Phys. **82**, 1287 (2010).

[2] A. Demircan and G. Steinmeyer, Controlling light by light with an optical event horizon, Phys. Rev. Lett. **92**, 163901 (2011).

- [3] T. G. Philbin, C. Kuklewicz, S. Robertson, S. Hill, F. König, and U. Leonhardt, Fiber-optical analog of the event horizon, *Science* **319**, 1367 (2008).
- [4] K. E. Webb, M. J. Erkintalo, Y. Xu, N. Broderick, J. M. Dudley, G. Genty, and S. G. Murdoch, Nonlinear optics of fibre event horizons, *Nat. Commun.* **5**, 4969 (2014).
- [5] R. Driben, A. V. Yulin, A. Efimov, and B. A. Malomed, Trapping of light in solitonic cavities and its role in the supercontinuum generation, *Opt. Express* **21**, 19091-19096 (2013).
- [6] S. F. Wang, A. Mussot, M. Conforti, X. L. Zeng and A. Kudlinski, Bouncing of a dispersive wave in a solitonic cage, *Opt. Lett.* **40**, 3320 (2015).
- [7] T. Voytova, I. Oreshnikov, A. V. Yulin, and R. Driben, Emulation of FabryPerot and Bragg resonators with temporal optical solitons, *Opt. Lett.* **41**, 2442 (2016).
- [8] I. Oreshnikov, R. and Driben, and A. V. Yulin, Weak and strong interactions between dark solitons and dispersive waves, *Opt. Lett.* **40**, 2442 (2015).
- [9] I. Oreshnikov, R. and Driben, and A. V. Yulin, Interaction of high-order solitons with external dispersive waves, *Opt. Lett.* **40**, 5554 (2015).
- [10] A. V. Yulin, D. V. Skryabin, and P. St. J. Russell, Four-wave mixing of linear waves and solitons in fibers with higher-order dispersion, *Opt. Lett.* **29**, 2411 (2004).
- [11] A. Efimov, A. V. Yulin, D. V. Skryabin, J. C. Knight, N. Joly, F. Omenetto, A. J Taylor, P. St. J. Russell, Interaction of an optical soliton with a dispersive wave, *Phys. Rev. Lett.* **95**, 213902 (2005).
- [12] D. V. Skryabin and A. V. Yulin, Theory of generation of new frequencies by mixing of solitons and dispersive waves in optical fibers, *Phys. Rev. E* **72**, 016619 (2005).
- [13] A. Efimov, A. J. Taylor, A. V. Yulin, D. V. Skryabin, and J. C. Knight, Phase-sensitive scattering of a continuous wave on a soliton, *Opt. Lett.* **1**, 1624 (2006).
- [14] A. V. Yulin, L. R. Gorjao, R. Driben, and D. V. Skryabin, Tuning resonant interaction of orthogonally polarized solitons and dispersive waves with the soliton power, *Opt. Express* **22**, 10995 (2014).
- [15] A. Choudhary and F. Konig, Efficient frequency shifting of dispersive waves at solitons, *Opt. Express* **20**, 358 (2012).
- [16] S. F. Wang, A. Mussot, M. Conforti, A. Bendahmane, X. L. Zeng, and A. Kudlinski, Optical event horizons from the collision of a soliton and its own dispersive wave, *Phys. Rev. A* **92**, 023837 (2015).
- [17] G. P. Agrawal, *Nonlinear Fiber Optics*, 4th. Edition, Academic Press (2007).
- [18] N. Akhmediev and M. Karlsson, Magnus, Cherenkov radiation emitted by solitons in optical fibers, *Phys. Rev. A* **51**, 2602 (1995).
- [19] K. J. Blow, N. J. Doran, and D. Wood, Polarization instabilities for solitons in birefringent fibers, *Opt. Lett.* **12**, 202 (1987).
- [20] F. Luan, A. V. Yulin, J. C. Knight, and D. V. Skryabin, Polarization instability of solitons in photonic crystal fibers, *Opt. Express* **14**, 807 (2006).
- [21] N. Akhmediev and J. M. Soto-Crespo, Dynamics of solitonlike pulse propagation in birefringent optical fibers, *Phys. Rev. E* **49**, 5742 (1994).
- [22] J. M. Soto-Crespo, N. Akhmediev, and A. Ankiewicz, Stationary solitonlike pulses in birefringent optical fibers, *Phys. Rev. E* **51**, 3547 (1995).
- [23] Y. Baradand, and Y. Silberberg, Polarization Evolution and Polarization Instability of Solitons in a Birefringent Optical Fiber, *Phys. Rev. Lett.* **78**, 3290 (1997).
- [24] D. C. Hutchings and J. M. Arnold, Polarization stability of solitons in birefringent optical fibers, *J. Opt. Soc. Am. B* **16**, 513 (1999);